Metal to Composite

D. Villadsen, F. Prieto Viejo, J. Mato Sanz, P. J. Jaume Camps and S. Hermansen

Department of Materials and Production, Aalborg University
Fibigerstraede 16, DK-9220 Aalborg East, Denmark
Email: {dvilla15, jmatos18, fpriet18, pjaume18, sherma15}@student.aau.dk,
Web page: http://www.mechman.mp.aau.dk/

Abstract
This work concerns redesign of a centrifugal pump. The motivation for the redesign is to change the material from metal to composite in order to eliminate the main problem of corrosion. The material chosen to apply to the pump is a discontinuous fiber reinforced polymer material PPS-GF40. The behavior of such a material is anisotropic in nature and, as opposed to continuous fibers, difficult to design. Material modeling is done in order to characterize this behavior, which entails fiber orientation prediction, micromechanical modeling of the stiffness and strength. A laminate approximation is also proposed in order to improve the computational speed in the following optimization. Topology optimization is then applied in order to gain an initial design with the optimal distribution of the new material. Inadequacy in the topology optimization method used however lead to the development of further optimization models, which were applied to treat the problem with the stress in the tongue and eigenfrequencies of the pump. A final design was proposed, which is made for injection molding, has characterized its theoretical stiffness and strength properties, eliminated corrosion and reduced the stress by a factor of 6.6.

Keywords: Centrifugal pump housing, Redesign, Discontinuous fiber reinforced composite, Material modeling, Structural optimization, Topology optimization

1. Introduction

Many pumps are designed today with metal materials such as steel, cast iron, bronze, etc. A problem with these materials is that they can corrode, which severely impacts the mechanical performance of the material and thereby its life time. This is also the case with the pump housing for the NB 65-200 centrifugal pump made of cast iron, manufactured by company Grundfos.

Composites are widely used today due to their ability to be tailored for a specific purpose. Composites can be made out of two materials from different material groups. A common combination in engineering applications is plastic, reinforced with ceramic fibers. By using this combination, it is possible to eliminate the problem with corrosion, as neither of the materials corrode. Due to this, Grundfos proposed a project, which entails redesigning the pump housing such that the cast iron material can be replaced by a fiber reinforced polymer (FRP).

As Grundfos is implementing more complex manufacturing methods, which allow for decreased manufacturing time, increased automation and creation of complex geometries, it is desired to design for manufacturing with one of these methods. The design will therefore be developed for injection molding. Injection molding allows for complex shapes to be manufactured by injection of a molten (reinforced) plastic into a mold.

In general, composite materials can be grouped into two different variations; continuous fiber reinforced composite materials (CFRC) and discontinuous fiber reinforced composite materials (DFRC). When using injection molding, the fibers are supplied to a rotating screw, which mixes the plastic material with the fibers. No matter if either continuous fibers or discontinuous fibers are used, the fibers will be cut into small pieces during the injection process. This means that the design must be made with DFRC if injection molding is used. Although the fraction of fibers and matrix is the same for a CFRC and a DFRC, the properties will be way different. CFRC are commonly used in applications where superior strength or stiffness are required in known directions, allowing for alignment of the fibers in this direction. DFRC, however, cannot achieve the same amount of strength and stiffness, even if the material is completely aligned in the same direction as a CFRC. Furthermore, DFRC will have a very complex orientation state due to the injection molding process. A model must therefore be developed, which can predict the orientation, stiffness and strength of the material.

The new material utilized will exhibit a very different behavior compared to the previous one - most notably, it will go from being isotropic to anisotropic. Therefore, to have an idea about the new distribution of material, topology optimization will be performed on the design. This optimization will be conducted using the commercial program ANSYS Workbench. However, as the topology optimization module in ANSYS has limitations, post treatment will be done by performing detailed design of the areas, which were not adequate from the topology optimization results.

1.1 Analysis of the Existing Design

The NB 65-200 pump is a single stage, non-self-priming, end suction, volute centrifugal pump. A 3D model of the pump is shown in Fig. 1.

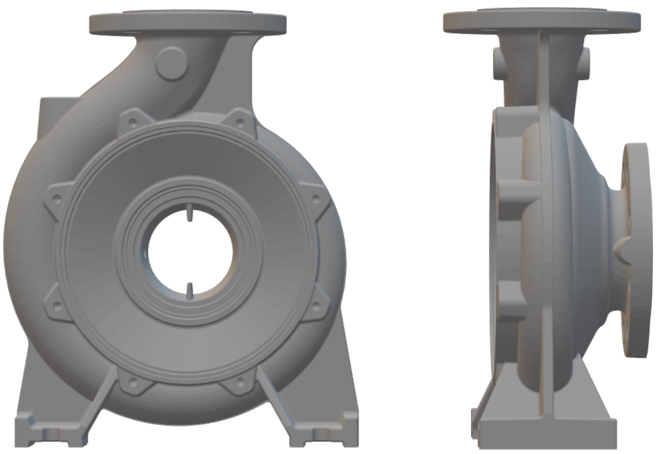

Fig. 1 3D CAD model of the NB 65-200 pump. Left side shows the rear of the pump with the motor flange, while the right side illustrates the side of the pump.

The flange with bolt holes shown on the left of Fig. 1 is the mounting flange for the motor. The pump is connected to a piping system through the inlet and outlet, which are the right and top flanges, respectively, on Fig. 1. The pump housing is fixed to the ground by bolts.

In order to identify the structural critical areas of the pump, a Finite Element Analysis (FEA) is performed on the pump using the commercial program ANSYS Workbench. The first analysis is that of a static structural analysis. This is performed in order to find the weakest area of the pump, i.e. the location with highest maximum principal stress. The pump will be modeled as having a rigid fixation to the ground and loaded with an operating pressure as well as the mass of the motor. When this pump is tested, the test is performed using a pressure of 24 [bar], which adds a safety factor to the operating pressure. As can be seen on the CAD model illustrated in Fig. 1, there are openings, where the motor, inlet pipe and outlet pipe should be mounted. Applying only the pressure to the inside of the pump housing is not sufficient for representing the load case, since the pressure also acts on the openings, while the pump is in operation. Therefore, the pressure is balanced by applying compensating forces on each opening. These balancing forces are found by multiplying the operating pressure by the opening area.

To best capture the complex stress state, quadratic elements are used. At first, a coarse mesh is used in order to get an overview of the stress state, and find the most critical areas, whereafter subsequent model refinement can be done. The results from the presented model are shown in Fig. 2

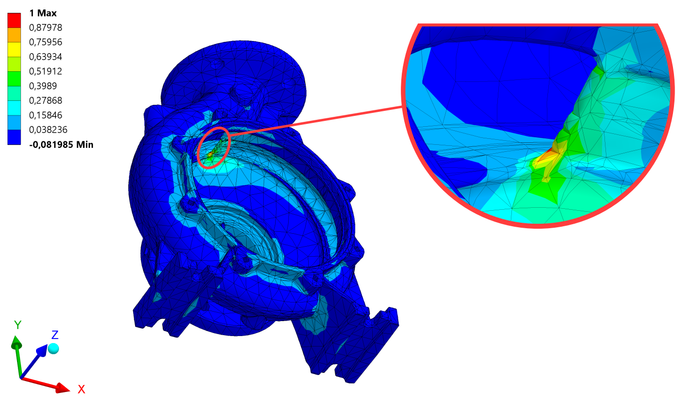

Fig. 2 Illustration of the stress state in the pump. It can be observed, that by far the most critical point is the volute tongue. The stresses have been normalized with the maximum value.

Having identified the most critical point to be in the edge shown in Fig. 2, which is termed the volute tongue, mesh refinement can be done. As only the student version of ANSYS was available with a limit of 256,000 nodes, a submodel of the tongue is performed. By doing this, the rest of the pump can be meshed with a relatively fine global mesh, while still capturing the high stress from the stress concentration in the volute tongue using a very fine mesh. The results are shown in Fig. 3.

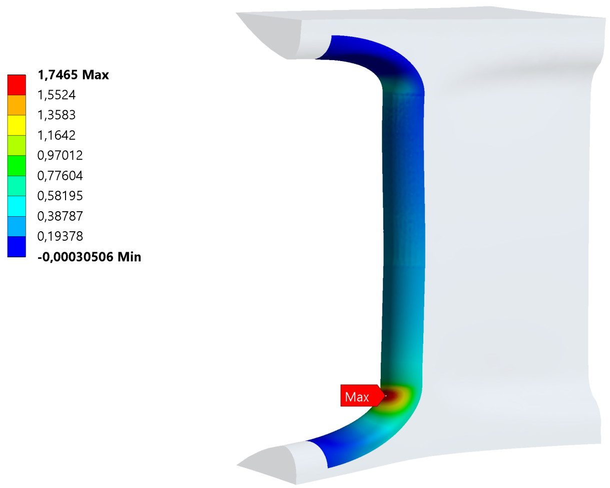

Fig. 3 The stresses in the submodel. The values have been normalized with respect to the maximum stress from Fig. 2.

Due to confidentiality agreements, the results cannot be stated, however, it is recognized from this submodel that the stress is many times the material strength, which is a problem, that has to be treated in the redesign.

Another important factor for the failure of the pump is the eigenfrequencies of the pump. The motor mounted to the pump housing runs at a constant frequency of either 50 or 60 [Hz] depending on the motor. The pressure in the pump is created by a rotating impeller inside the pump housing. The impeller of this pump has six blades, and the impeller increases the operating frequency due to the blade's trailing edge passing the volute tongue. This is termed the blade-passing frequency. The blade passing frequency therefore becomes 300 or 360 [Hz] depending on the motor.

The eigenfrequency analysis is also performed using ANSYS Workbench. Besides the mass of the motor, the mass of the impeller and the mass of the water inside the pump are also included in the analysis. The mass of the water is added by increasing the density of the material, and thereby assuming that it acts evenly throughout the pump. The mass of the motor is taken as the motor with the highest mass in the Grundfos catalogue. The analysis is conducted using the same mesh as in the static structural analysis. The resulting first three eigenfrequencies are shown in Tab. I.

Mode	1	2	3
Frequency [Hz]	106.16	480	623.44
Type	Bending x-axis	Bending z-axis	Torsional

Tab. I The three first eigenfrequencies of the pump with description of the eigenmode. These three eigenfrequencies are the most critical as they are closest to the operating frequency range. For coordinate system, see Fig. 2.

Some inaccuracy in the model is expected due to the fact that the piping adds additional stiffness to the system, added mass from the surrounding water, i.e. if the pump is submerged in water, and also if the analysis is conducted with a smaller motor, which results in a smaller mass, is not taken into account.

2. Material Modeling

The anisotropy the material exhibits is a consequence of the presence of the fibers in the matrix. The fiber dispersion is characterized by the particles being aimlessly dispersed due to the injection molding. On the other hand, the orientation tends to follow a pattern which is heavily influenced by the flow conditions and the geometry of the part. Thus, a model, which can predict the behavior of the anisotropic material, is studied.

2.1 Fiber Orientation Prediction

In the continuum, fiber orientation is described by a probability distribution function $\psi(\mathbf{p})$, where $\mathbf{p}$ is the direction vector of the fiber. For a planar flow state, $\mathbf{p}$ is described in terms of the orientation angle ϕ

$$\begin{aligned} p_1 &= \cos\phi \\ p_2 &= \sin\phi \end{aligned} \tag{1}$$

As a consequence of having a concentrated suspension (40% of fiber volume fraction), the interaction between fibers must be accounted for with the Folgar-Tucker model [1], where the rotational speed $\dot{\phi}$ is calculated. This is used in the continuity equation (2) to calculate the rate of change of the distribution function through a control volume, as:

$$\frac{\partial\psi}{\partial t} = -\frac{\partial}{\partial\phi}(\psi\dot{\phi}) \tag{2}$$

The probability function can be presented with an orientation tensor a_{ij}, defined as the average of all directions of $\mathbf{p}$ and weighted by ψ [1].

$$a_{ij} = \int p_i p_j \psi(\mathbf{p}) \mathrm{d}\mathbf{p} \tag{3}$$

Thus, (2) can be expressed in terms of a_{ij}, and the rate of change of a_{ij} can be obtained. Therefore, the continuity equation is to be solved numerically for the injection process. The software used for this purpose is Moldex3D, a finite element program in which the injection is simulated, and from where a_{ij} is calculated element-wise at each time step.

2.2 Micromechanics

Taking offset in the material properties corresponding to all the fibers aligned, the resultant properties of any fiber orientation and fiber probability distribution can be calculated. In this project, the procedure explained in [2] is followed. The principle is to average the properties of the unidirectional material along all the possible orientations weighted by the probability of orientation. The averaged stiffness tensor of the material is defined as

$$\langle C_{ijkl} \rangle = \int \int \psi(\mathbf{p}) x_{ip} x_{jq} x_{kr} x_{ls} C_{pqrs} d\mathbf{p} \quad (4)$$

where x_{ij} is the coordinate transformation tensor $\psi(\mathbf{p})$ is the orientation function, $\langle - \rangle$ means orientation averaged magnitude and C_{pqrs} is the stiffness tensor.

As a result of the procedure followed to characterize the fiber orientation and the stiffness, the resultant material will be an orthotropic material for each point with varying properties along the continuum. This method is used for every 3D stiffness calculation.

2.3 Laminate Approximation

Although the previous method represents a good definition of the material properties, it is a costly method, which requires a flow analysis and a micromechanical postprocessing for each change of the design. Any iterative design process demands a flexible model on the initial stages which allows a quicker development.

After studying the patterns of the components manufactured through injection molding, it turns out that there is a common distribution of fiber orientation though the thickness. Three major regions can be clearly separated: two regions close to the walls of flow-oriented fibers and a core in between with a more random orientation, as seen in Fig. 4.

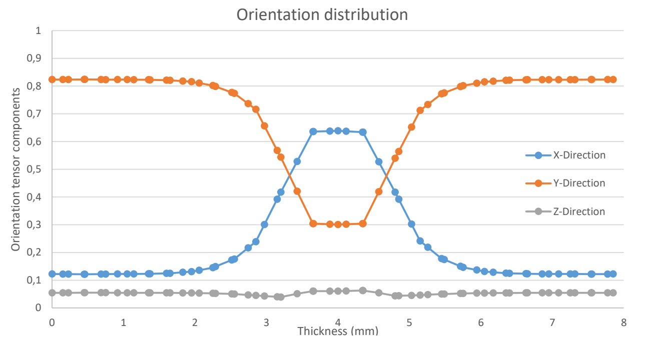

Fig. 4 Fiber orientation distribution of a component simulated in Moldex3D.

Being aware of this, it was decided to approximate the injected components to a three-layer laminate. The core has the properties of completely random distribution of fibers in the plane perpendicular to the thickness direction. The face sheets are symmetric and have the properties of flow-oriented fibers. Knowing the material properties and the average direction of the flow in a region, the only variable left is the relation between the thickness of the face sheets and the core. For this calculation, a series of plates with different thicknesses are injected in Moldex3D and the variation of the orientation probability is extracted. Then, the plate laminate stiffness matrix is calculated through the First order Shear Deformation Theory (FSDT). The laminate stiffness matrix of the equivalent three-layered plates is defined as a function of the thickness of the face sheets. Through the least-squares method, this thickness is calculated by the optimization problem in equation (5) for each total thickness.

$$\begin{aligned} \text{Minimize:} \quad & f(\mathrm{h}) = \textstyle\sum_{i=1}^{8} \sum_{j=1}^{8} \left(C_{ij}^{\mathrm{mold}} - C_{ij}^{\mathrm{eq}}(\mathrm{h}) \right)^2 \\ \text{Subject to:} \quad & -h \leq 0 \\ & h \leq t \end{aligned} \quad (5)$$

Where C_{ij}^{mold} is the plate stiffness matrix of the data obtained from Moldex3D, C_{ij}^{eq} is the plate stiffness matrix of the equivalent laminate, h is the thickness of the face sheets and t is the total thickness of the plate.

Finally, the laminate approximation is validated in ANSYS by comparing the results with the ones with 3D fiber orientation data imported from Moldex3D. The setups used are cantilever beam under tension and three-point bending. The results compared are maximum displacement and maximum principal stress in static structural analysis and three lower eigenfrequencies in an eigenfrequency analysis. The results are compared in terms of relative error in Tab. II and Tab. III.

Plates	Max. disp.	1st mode	2nd mode	3rd mode
2x80x200	9%	3%	2%	3%
4x80x200	1%	0%	4%	1%
6x120x240	1%	1%	4%	1%
7x160x350	3%	0%	3%	1%
8x160x320	2%	1%	3%	1%

Tab. II Relatives errors of the considered variables between the plates for the cantilever beam model. *Max. disp.* means maximum displacement.

Plates	Stress	Max. disp.	1st mode	2nd mode	3rd mode
2x80x200	5%	6%	0%	2%	1%
4x80x200	2%	0%	3%	2%	2%
6x120x240	0%	1%	2%	0%	2%
7x160x350	0%	1%	2%	1%	3%
8x160x320	1%	2%	1%	3%	2%

Tab. III Relative errors of the considered variables between the plates for the three-point bending model. *Max. disp.* means maximum displacement.

2.4 Anisotropic Failure Criteria

The orientation of the fibers and the stiffness of the anisotropic material have now been characterized in every finite element. It is therefore desired to characterize the strength in order to evaluate failure of the pump. To do this, the longitudinal and transverse strength of the unidirectional DFRC must be determined. Following the approach of [3], the longitudinal strength σ_{cL} can be determined as

$$\sigma_{cL} = V_f \sigma_f \left(1 - \frac{L_c}{2L}\right) + \sigma'_m (1 - V_f), \text{ for } L_c \leq L \tag{6}$$

$$\sigma_{cL} = V_f \sigma_f \left(\frac{1}{2L_c}\right) + \sigma'_m (1 - V_f), \text{ for } L_c > L \tag{7}$$

Here, σ_f is the fiber strength, σ'_m is the matrix stress at fiber failure, V_f is the fiber volume fraction, L is the length and L_c is the critical length, which is found as:

$$L_c = \sigma_f \frac{d}{2\tau} \tag{8}$$

where d is the fiber diameter, and τ is the interfacial shear strength. By assuming a strong interfacial bond between fiber and matrix, the transverse strength σ_{cT} is equal to the strength of the matrix, σ_m i.e.

$$\sigma_{cT} = \sigma_m \tag{9}$$

In the case of isotropy of the matrix and strong interfacial bonds, the shear strength can be determined by the von Mises criterion

$$\tau = \frac{\sigma_m}{\sqrt{3}} \tag{10}$$

A popular and effective choice of failure criterion for CFRC materials is the Tsai-Wu failure criterion [4]. This criterion can also be formulated for DFRC by including the fiber orientation tensor. The general Tsai-Wu for a 3D stress state is formulated in contracted notation as:

$$F_i \sigma_i + F_{ij} \sigma_i \sigma_j = 1 \tag{11}$$

Indicating that failure occurs if the equation is equal to unity. The stresses σ_i and σ_j are the applied stresses in contracted notation. The Tsai-Wu strength tensors F_i and F_{ij} are given by the strength of the material. By considering a composite with fibers perfectly aligned along one axis, the material will behave transversely isotropic. The definition of the strength tensors of the transversely isotropic DFRC, $F_i = \{0\}$ and F_{ij} will have the following nonzero entries

$$\begin{aligned} &F_{11} = \frac{1}{\sigma_{cL}^2}, \quad F_{12} = F_{21} = -\frac{1}{2\sigma_{cL}^2} \\ &F_{22} = \frac{1}{\sigma_{cT^2}}, \quad F_{23} = F_{32} = -\frac{1}{2}\left(\frac{2}{\sigma_{cT}^2} - \frac{1}{\sigma_{cL}^2}\right) \\ &F_{33} = \frac{1}{\sigma_{cT^2}}, \quad F_{44} = \left(\frac{4}{\sigma_{cT}^2} - \frac{1}{\sigma_{cL}^2}\right) \\ &F_{55} = F_{66} = \frac{1}{\tau^2}, \end{aligned} \tag{12}$$

To take the fiber orientation into account, the fiber orientation tensor must be included. The procedure is to average the Tsai-Wu strength tensor, by the use of the fiber orientation tensor [1]. In expanded notation, this results in

$$\begin{aligned} \langle F \rangle_{ijkl} &= B_1 a_{ijkl} + B_2 (a_{ij}\delta_{kl} + a_{kl}\delta_{ij}) \\ &+ B_3 (a_{ik}\delta_{jl} + a_{il}\delta_{jk} + a_{jl}\delta_{ik} + a_{jk}\delta_{il}) \\ &+ B_4 (\delta_{ij}\delta_{kl}) + B_5 (\delta_{ik}\delta_{jl} + \delta_{il}\delta_{jk}) \end{aligned} \tag{13}$$

Here, a_{ijkl} is the fourth order orientation tensor, δ_{ij} is the Kronecker delta and $B_{1,\ldots,5}$ are constants directly related to the tensor being averaged. After calculation of $\langle F \rangle_{ijkl}$, the strength tensor can be contracted and is then ready for use in (11). However, to make (11) scalable, it must be linearized, since it is nonlinearly dependent on the stresses in its traditional form. This is done by introducing the variable γ and by rewriting (11) into a polynomial expression as follows:

$$\gamma^2 F_{ij} \sigma_i \sigma_j + \gamma F_i \sigma_i - 1 = 0 \tag{14}$$

From which γ can be solved. The failure index F_I is then defined, using γ as:

$$F_I = \frac{1}{\gamma} < 1 \tag{15}$$

3. Structural Optimization

In the following, the structural optimization methods used, and the results obtained, will be described.

3.1 Topology Optimization

A topology optimization is performed on the pump, having applied the new material. As the pump will be manufactured using injection molding, which is excellent for manufacturing highly complex shapes, it is of much interest to find the optimum placement of material, no matter how complex it is. In order to perform the topology optimization, the CAD model of the pump housing is enclosed by material, as the topology optimization method is not able to place material, but to find the optimum distribution in an existing domain. This is illustrated in Fig. 5.

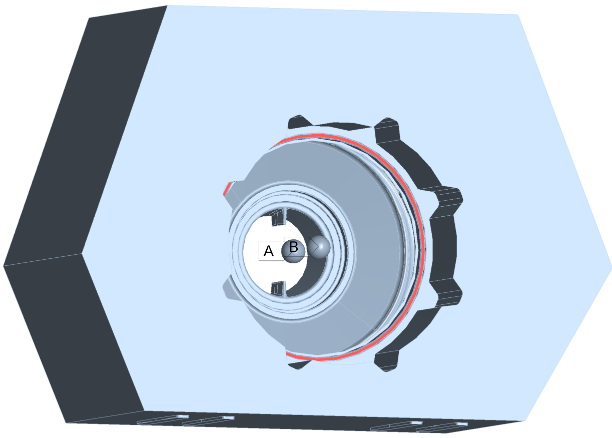

Fig. 5 Rear side of the pump housing wrapped in material. The spheres illustrated by A and B are the masses of the impeller and motor respectively.

As the topology optimization is conducted using ANSYS Workbench some limitations are present. The topology module in ANSYS Workbench only has the Solid Isotropic Material with Penalization (SIMP) method available, which is not applicable to anisotropic materials. It is therefore desired to perform the topology optimization as an approximation to the optimal geometry, and then post-process the results to achieve a feasible design.

The topology optimization is done in FEM form. The SIMP scheme used, presented in [5][6], is a simple density-based topology optimization method. The method entails solving the 0-1 problem of topology optimization by introducing a continuous density variable $\rho(\mathbf{x})$, which simplifies the problem by allowing intermediate values between 0 and 1 as:

$$E_e(\rho_e) = \rho_e E_e^* \tag{16}$$

Here, E_e is the stiffness of a finite element and E_e^* is the stiffness of the material. The continuous density variable, ρ_e, is here defined for each element. As only the values 0 and 1 are permissible, the intermediate values are penalized by inclusion of a penalty factor p, making 0 and 1 the most efficient values for the algorithm to choose.

$$E_e = \rho_e^p E_e^* \tag{17}$$

The value of p is usually set to 3 [7].

Constraints are then formulated with respect to stress and eigenfrequency. The stress constraint is formulated using the method proposed by [7]. This is done in order to avoid the singular optima problem occurring when using stress constraints, as elements that have zero density may still have finite stress values. The solution proposed is to relax the problem by introducing a new variable q, which replaces p in the stress constraint expression, where $q < p$. By applying this, the stress constraint is formulated in finite element form as

$$\sigma_{VM,e} = \rho_e^q \sigma_{Y,e} \tag{18}$$

The stress $\sigma_{Y,e}$ is the yield stress of the material in an element and $\sigma_{VM,e}$ is the von Mises stress computed in the center of the element.

In this formulation, the problem becomes a very large scale problem due to the stresses being formulated as local constraints, creating a constraint for each element in the model. In order to make the algorithm more efficient, the constraints are therefore aggregated into a global constraint. This is done by e.g. the P-norm method

$$g_{VM} = \left(\sum_{e=1}^{n_e} (\sigma_{e,VM})^P \right)^{1/P} \tag{19}$$

Here, P is a penalization parameter. The larger the value of P, the more accurate the constraint will be. However, large values of P are computationally inefficient. Therefore, the idea of adaptive constraint scaling outlined in [8] where a scaling parameter c is multiplied by the global constraint. The stress constraint can thereby be formulated as:

$$\begin{gathered} max(\sigma_{VM}) = c g_{VM} \\ c^i = \alpha^i \frac{max(\sigma_{VM})^{i-1}}{g_{VM}^{i-1}} + (1-\alpha^i) c^{i-1} \\ \alpha = [0,1] \end{gathered} \tag{20}$$

Here, i is the current iteration number and α is a damping constant, which value is chosen in order to prevent c from oscillating.

The optimization problem can then be formulated. In terms of minimizing volume subject to stress constraints and eigenfrequency constraints, the formulation is

$$\begin{aligned} \underset{\rho(\mathbf{x})}{\text{minimize}} \quad & V = \frac{1}{V^*}\sum_{e=1}^{n_e} v_e \rho_e \\ \text{subject to} \quad & \frac{c^i g_{VM}(\mathbf{x})}{\sigma_Y} - 1 \leq 0 \\ & \omega_{d1} \leq \omega_i \leq \omega_{d2} \\ & E_e = \rho_e^p E_e^* \\ & 0 < \rho_{min} \leq \rho_e \leq 1 \end{aligned} \tag{21}$$

Here, V is the volume, V^* is the reference volume, v_e is the volume of an element, ω_i is an eigenfrequency, ω_{d1} and ω_{d2} are limits on the eigenfrequency. A lower bound on the density variable ρ_{min} is included, which ensures that the stiffness matrix does not become singular.

Results

Many optimization setups are investigated to determine, which will provide the best results. The initial approach is to run volume minimization subject to stress constraints only, then subject to eigenfrequency constraints only and then make an interpretation of the resultant geometry. The results of the stress constrained topology optimization are shown in Fig. 6. The next

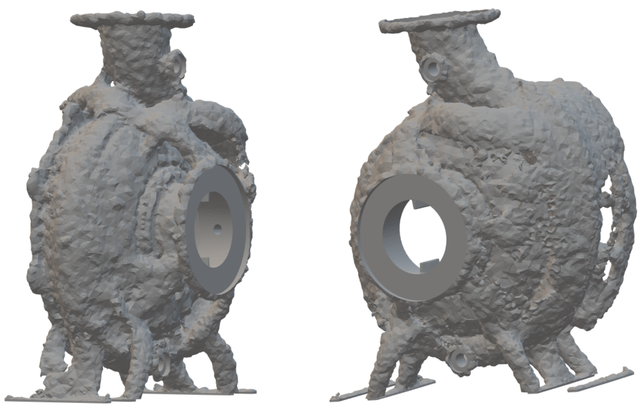

Fig. 6 Results from the stress constrained topology optimization.

optimization run, which was done with eigenfrequency constraints, was unable to converge. Therefore, a multi-objective formulation is used instead, where the volume is minimized and the third eigenfrequency is maximized. The objective is subject to a stress constraint and two eigenfrequency constraints of limiting the frequencies to be at least 30% below the operating frequency. The results are shown in Fig. 7.

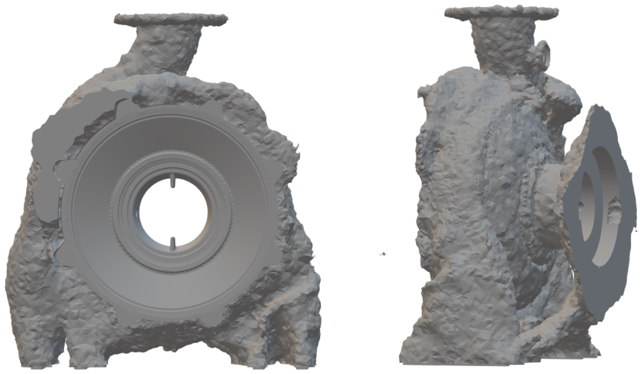

Fig. 7 Results from the multi-objective optimization.

These results provide a starting point for further design.

3.2 Thickness Optimization

The resultant geometries from the topology optimization analyses provide an idea on how the mass should be distributed in the structure to achieve the required goals. A postprocessing of the results is necessary to obtain a geometry subject to manufacturing constraints and suitable for further analyses. One of the main manufacturing constraints when designing specimens, which are to be injection molded, is avoiding changes in thickness through the same surface. This is to avoid shrinkage and warpage. Therefore, the resulting interpreted geometries should have constant surface thickness in all the reinforcements.

This second step of the optimization is supposed to give a better representation of a real specimen. For this purpose, a FEM model is done using the module ANSYS Composites Prep/Post (ACP) for defining the orthotropic properties and fiber orientation in each region. The input of this module is a geometry composed of surface bodies. The fiber orientation is obtained from a qualitative analysis of the flow. Then, a solid model is created, as the one shown in Fig. 8, by extruding the input surfaces.

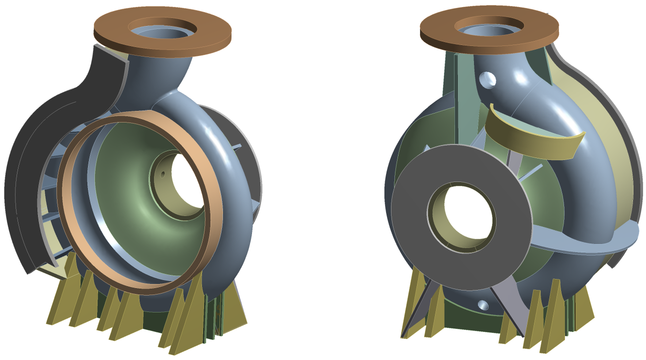

Fig. 8 Example of a geometry generated in ACP.

After creating the full model, the thickness of each surface is defined as a parameter in ANSYS Workbench in order to perform different response studies and use optimization algorithms in the design process.

The module ACP is intended to be used for laminated composites. Thereby, it makes it very complicated to represent complex 3D geometries. The critical region in terms of stress is the tongue. Therefore, this model will only be used to optimize the part in terms of eigenfrequencies.

4. Detailed Design

In this section, the detailed redesign stage, which involves design for strength and design for eigenfrequencies alongside with their corresponding results, will be presented.

4.1 Design for Strength

The detailed design will have as main objective to downsize the stress at the volute tongue, which is approximately seven times the tensile strength of the new material, until a value lower than this one, which might make the design feasible for structural purposes. This redesign stage will comprise two phases; the first one consists of an optimization of the existing volute tongue geometry, and if the target stress is still not reached, a second phase involving major geometrical changes following the engineering intuition will be done. The first optimization is carried out changing the basic geometry of the tongue, which are the three roundings that conform this part, see Fig.9. Different bounds are fixed for each rounding and a Surface Response Optimization (using a Multi-Objective Genetic Algorithm) is executed with the aim of minimizing stress until an optimum geometry is obtained. The values for the optimized tongue are: 4.8 [mm] (side rounding) and 0.2 [mm] (for both upper and lower roundings). The value of the stress in the tongue is lowered approximately a 50 % of the initial value.

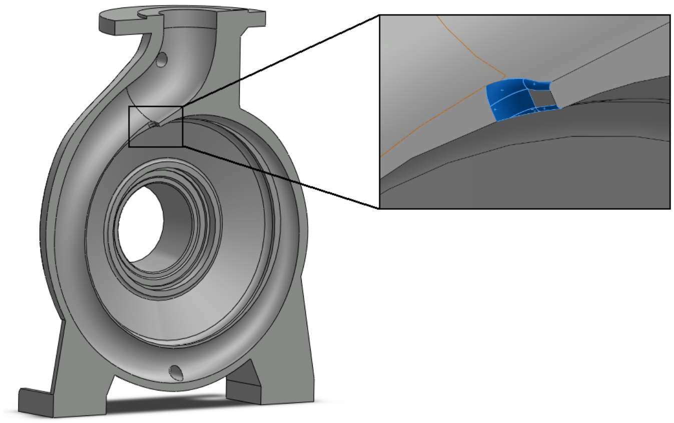

Fig. 9 Roundings of the volute tongue chosen for the optimization.

This reduction of stress is not enough to comply with the requirements of the redesign, which suggests that the volute tongue should be treated alongside with the whole pump in the design. Subsequently, an intuitive redesign will be accomplished to solve the issue. Before modifying the pump housing any further, a closer look at the deformed state of the pump is taken to identify the cause of the stress accumulation in the tongue. This further investigation on the deformation made clear that the walls of the pump expand outwards, see Fig. 10. As a result of this phenomenon, the tongue, which acts like a joint between both walls, carries all the stresses caused by this deformation. Thereby the stress in the tongue is not only dependent on the geometry of this part, but of the entire pump.

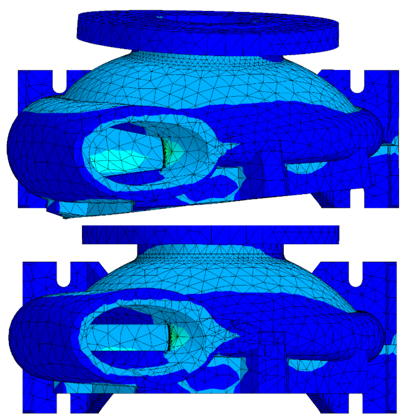

Fig. 10 Deformed shape of the pump (up), undeformed shape of the pump (down).

This observation clearly indicates that a reinforcement along the shoulder of the pump (which undergoes the highest deformation, see Fig. 10) has to be implemented for preventing expansion of the pump, see Fig. 11. An iterative process, adding ribs and changing the shape and configuration of the reinforcements, takes place until a feasible model that can withstand the load case stated is reached.

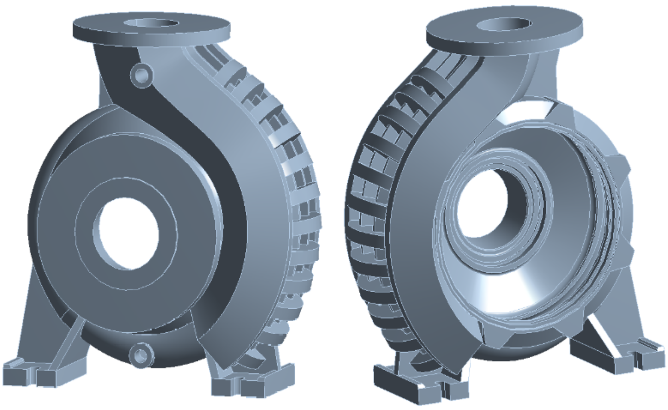

Fig. 11 Pump housing reinforced.

4.2 Design for Eigenfrequencies

After creating a geometry from the results of the topology optimization, a thickness optimization is run in order to fulfill the modal requirements. This optimization failed, which shows that the initial interpreted geometry is not feasible, the second and the third eigenfrequencies are not separated enough to maintain both on the safe side, the second below the blade-passing frequency and the third one above. Consequently, it is decided to start an iterative design process in which other results from the topology optimization and engineering intuition are used to perform the necessary changes in the geometry.

Two new variables are defined to track the design process:

- Objective: The difference between the second and third eigenfrequencies measured as a percentage of the required difference.
- Improvement: The change of the objective, defined above, between following subiterations.

An iteration is a step where the resultant design is satisfactory, and a subiteration is a step when the output is unsatisfactory. The result history of the design process is shown in Fig. 12. The design was guided by the study of the mode shapes, trying to stiffen the third mode while leaving the second mode unaltered.

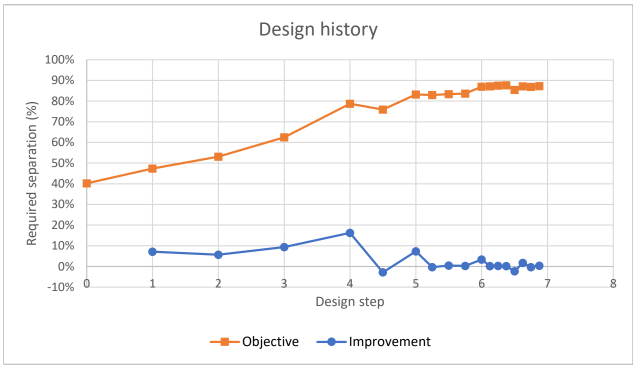

Fig. 12 History of the variables used to track the design process.

It can be seen that the initial changes improved the design rapidly but only caused minor changes during the last steps. When, after several steps, the design result remains the same, the iterative design process is considered finished. Then, the resultant model is subject to a thickness optimization to separate the second and the third eigenfrequencies as much as possible. The best candidate found is:

	1st mode	2nd mode	3rd mode
Frequency [Hz]	188.4	209.4	413.6

Tab. IV Results from the thickness optimization.

4.3 Final Design

After optimization has been done for the stress and eigenfrequency separately, the results from these are combined to a final design. As a result of the combination of the optimized results, the final geometry is modeled, such that it should fulfill the requirements that both designs demand. The new design is illustrated in Fig. 13.

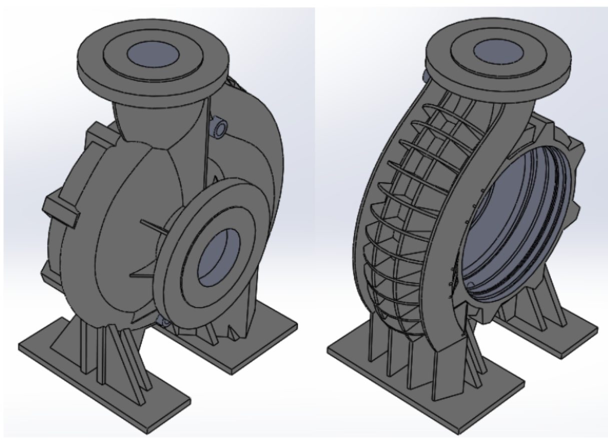

Fig. 13 Model of the final design.

However, after analyzing the injected pump, it is noticed that both requirements cannot be achieved under the same model. Thus, it is chosen to comply with the strength, since the reduction obtained, a reduction of a factor of 6.6, is substantially better than the results obtained for the eigenfrequencies. The stress has been evaluated in the Tsai-Wu failure criterion established. The failure in the tongue is illustrated in Fig. 14.

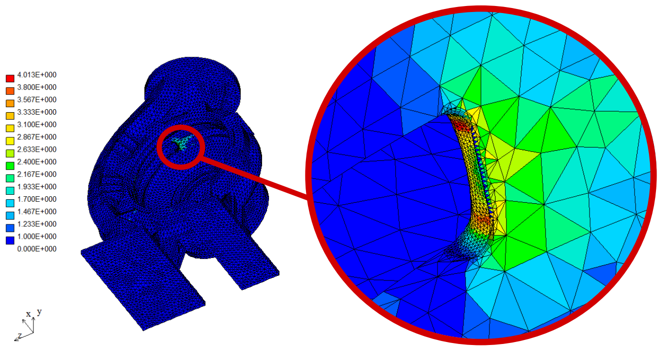

Fig. 14 The failure index in the tongue.

It can be noted, that the stress in the tongue still fails. However, by reducing the safety factor, i.e. such that the operating pressure is used, or by investigating, if the orientation of the fibers can be improved in the tongue, this problem could be resolved.

The eigenfrequencies are shown in Tab V.

	2nd mode	3rd mode	4th mode
Frequency [Hz]	174	300	423

Tab. V Eigenfrequencies of interest of the final design.

Small changes to the geometry to push the 3rd eigenfrequency off the operating frequency is, as observed, required. Additionally, harmonic analysis could help establish, how close the eigenfrequency can be allowed to be to the operating frequency values.

5. Conclusion

This project concerns changing the material of a pump housing from metal to composite in order to eliminate the problem of corrosion. Material modeling of the PPS-GF40 material was done. Here, the stiffness and strength of the anisotropic material were characterized by the prediction of the fiber orientation state after injection molding simulations of the pump housing.

Topology optimization was performed on the design, using the new material, however, the topology optimization method was inadequate, as it was based on isotropic materials. Postinterpretation of the generated design was therefore done to comply with the requirements.

From the interpretation of the topology optimization geometry, further design and parametric optimization for the stress state in the pump housing's critical point, the tongue, and for the pumps eigenfrequencies were done. The findings were put together in a final design proposal. In this design, the stress was reduced by a factor of 6.6 in the tongue. The final proposed design did not comply for eigenfrequencies, however, as one mode was critical when compared to the operating frequency. It was found, that a compromise had to be made between to move this eigenfrequency away from the operating frequency, as this would increase the stress.

Acknowledgement

The authors of this work gratefully acknowledge Grundfos for sponsoring the 7th MechMan symposium.

References

[1] S. G. Advani and C. L. Tucker, "The use of tensors to describe and predict fiber orientation in short fiber composites," Journal of Rheology Volume 31, Issue 8, 1987.
[2] J. Schjødt-Thomsen and R. Pyrz, Continuum Micromechanical Modelling of Composites and Cellular Materials, Part 1: Elasticity. Aalborg Universitetsforlag, 2003.
[3] F. V. Hattum and C. Bernardo, "A model to predict the strength of short fiber composites," Polymer Composites Volume 20, Issue 4, 1999.
[4] S. W. Tsai and E. M. Wu, "A general theory of strength for anisotropic materials," Composite Materials Volume 5, 1971.
[5] M. P. Bendsøe, "Optimal shape design as a material distribution problem," Structual Optimization Volume 1, vol. 1, pp. 193–202, 1989.
[6] M. Bendsøe and O. Sigmund, Topology Optimization - Theory, Methods and Applications. No. ISBN: 3-540-42992-1, Springer, 2003.
[7] M. Bruggi, "On an alternative approach to stress constraints relaxation in topology optimization," Struc Multidisc Optim Volume 36, 2008.
[8] C. Le, J. Norato, T. Bruns, C. Ha, and D. Tortorelli, "Stress-based topology optimization for continua," Struc Multidisc Optim Volume 41, 2010.